HHS Public Access

Author manuscript

Nano Lett. Author manuscript; available in PMC 2023 January 17.

Published in final edited form as:

Nano Lett. 2021 July 14; 21(13): 5850–5858. doi:10.1021/acs.nanolett.1c01840.

Nephrotoxicity Assessment with Human Kidney Tubuloids using Spherical Nucleic Acid-Based mRNA Nanoflares

Christian Wiraja,
Division of Renal Medicine, Department of Medicine, Brigham and Women's Hospital, Harvard Medical School, Boston, Massachusetts 02115, United States; School of Chemical and Biomedical Engineering, Nanyang Technological University, Singapore 637459, Singapore

Yutaro Mori,
Division of Renal Medicine, Department of Medicine, Brigham and Women's Hospital, Harvard Medical School, Boston, Massachusetts 02115, United States

Takaharu Ichimura,
Division of Renal Medicine, Department of Medicine, Brigham and Women's Hospital, Harvard Medical School, Boston, Massachusetts 02115, United States

Jangsun Hwang,
School of Chemical and Biomedical Engineering, Nanyang Technological University, Singapore 637459, Singapore

Chenjie Xu,
Department of Biomedical Engineering, City University of Hong Kong, Kowloon, Hong Kong SAR, China

Joseph V. Bonventre
Division of Renal Medicine, Department of Medicine, Brigham and Women's Hospital, Harvard Medical School, Boston, Massachusetts 02115, United States; Division of Engineering in Medicine, Department of Medicine, Brigham and Women's Hospital, Harvard Medical School, Boston, Massachusetts 02115, United States

Corresponding Authors Chenjie Xu – Department of Biomedical Engineering, City University of Hong Kong, Kowloon, Hong Kong SAR, China; chenjie.xu@cityu.edu.hk; **Joseph V. Bonventre** – Division of Renal Medicine, Department of Medicine, Brigham and Women's Hospital, Harvard Medical School, Boston, Massachusetts 02115, United States; Division of Engineering in Medicine, Department of Medicine, Brigham and Women's Hospital, Harvard Medical School, Boston, Massachusetts 02115, United States; joseph_bonventre@hms.harvard.edu.

Author Contributions

C.W., C.X., and J.V.B. conceived the idea for this study and designed the experiments with the assistance of Y.M. and T.I. C.W., Y.M., T.I., and J.H. performed the experiments. C.W. analyzed the data jointly with C.X. and J.V.B. C.W. and C.X. wrote the manuscript, which was revised and approved by all the authors.

Supporting Information

The Supporting Information is available free of charge at https://pubs.acs.org/doi/10.1021/acs.nanolett.1c01840.

Detailed experimental procedures; Figure S1-S7: additional NF characterization in solution, adenovirus-infected tubuloids, and AA and cisplatin-treated tubuloids; additional qPCR analysis data; Tables S1 and S2: list of anticancer drugs and oligonucleotides used (PDF)

The authors declare the following competing financial interest(s): J.V.B. and T.I. are co-inventors on KIM-1 patents that are assigned to MassGeneralBrigham. J.V.B. is cofounder and holds equity in Goldfinch Bio. The interests of J.V.B. were reviewed and are managed by BWH and Partners HealthCare in accordance with their conflict-of-interest policies. The other authors declare that they have no conflict of interest.

Abstract

Drug-induced nephrotoxicity represents an important cause of acute kidney injury with associated patient morbidity and mortality and is often responsible for termination of drug development, after extensive resource allocation. We have developed a human kidney tubuloid system that phenocopies, in 3D culture, kidney proximal tubules, a primary injury site of most nephrotoxicants. Traditional end point assays are often performed on 2D cultures of cells that have lost their differentiated phenotype. Herein, we pair a tubuloid system with Nanoflare (NF) mRNA nanosensors to achieve a facile, real-time assessment of drug nephrotoxicity. Using kidney injury molecule-1 (KIM-1) mRNA as a model injury biomarker, we verify NF specificity in engineered and adenovirus-transfected cells and confirm their efficacy to report tubular cell injury by aristolochic acid and cisplatin. The system also facilitates nephrotoxicity screening as demonstrated with 10 representative anticancer moieties. 5-Fluorouracil and paclitaxel induce acute tubular injury, as reflected by an NF signal increase.

Keywords

kidney organoids; spherical nucleic acid; nanoflare; clinical nephrotoxicity assessment; anticancer drugs; aristolochic acid; kidney injury molecule

The kidney has a specialized role in filtering substances from the blood to regulate the body's metabolic state and volume and electrolyte homeostasis. However, kidneys are particularly susceptible to toxicants as kidney blood flow represents approximately 20–25% of cardiac output and toxins filtered through the glomerulus can be concentrated while the filtrate is processed by the nephron.[1] Furthermore, toxicants can enter kidney epithelial cells from the blood. With its high metabolic activity associated with high levels of tubular secretion and reabsorption, kidney cells, particularly proximal tubule cells, are vulnerable to drug-induced injury.[2,3] Nephrotoxicity is estimated to account for up to 25% of significant adverse effects in current pharmacotherapy.[2] Drug-induced nephrotoxicity significantly impacts clinical outcomes including length of hospitalization, overall morbidity and mortality, and financial costs. When nephrotoxicity occurs in patients with cancer, who might require life-long drug intake, difficult decisions have to be made that often precipitate a trade-off between reducing ideal anticancer therapy or suffering the consequences of kidney failure with substantial impact on their quality of life.[4] Because acute kidney injury (AKI) has been recognized as an important predisposing factor to the development of chronic kidney disease, the importance of avoiding AKI is imperative.[5,6] There is a paucity of human tissue models to identify nephrotoxicity during drug development and to understand the cellular processes so that interventions can be introduced to prevent and treat nephrotoxicity. In addition, as we advance personalized therapy, understanding the genetic and nongenetic predispositions to nephrotoxicity of a particular agent can help to guide non-nephrotoxic therapies or use of patient-specific preventive approaches.[7]

Kidney tubuloids, a three-dimensional (3D) multicellular culture established from primary human tubular epithelium, is an alternative to 2D human cell systems, which are often dedifferentiated and do not phenocopy physiological proximal tubule functions and pluripotent stem cells-derived more complex kidney organoids.[8-10] Although organoids are

enriched in multiple kidney cells types their 3D architecture and variability can make quantitation of toxicity more challenging. The tubuloids are 3D cyst-like structures that maintain normal features of kidney proximal epithelial cells, such as membrane polarity, and are established from patient-derived tubular epithelial cells. Long-term polarized conformation of kidney tubuloids is evident with epithelial transporters present on the apical and basolateral membranes.[11] Their proliferation and biomarker expression profiles also suggest in vitro recapitulation of renal plasticity (regenerative responses) following injury.[9] Cisplatin was demonstrated to cause DNA damage and enhanced lactate dehydrogenase activity in cells dissociated from the tubuloids and placed on a chip platform.[9] Our laboratory has reported that palmitic acid bound to albumin (simulating a novel mechanism contributing to diabetic kidney disease), produces structural degradation of kidney tubuloids and secretion of pro-fibrotic factors, both of which were repressed by a small molecular inhibitor of palmitic acid-albumin uptake.[12] In addition, tubuloids derived from cystinotic or healthy patients enabled the validation of combination therapy in correcting altered cell phenotypes in cystinosis.[13]

Preclinical drug evaluation and clinical adaptation of kidney tubuloids to screen individualized risks of nephrotoxicity, however, are constrained by the limited number of patient-derived primary cells and the challenging cell expansion.[14] Current evaluation of tubuloid status relies on end-point molecular analyses like real-time quantitative polymerase chain reaction (RT-qPCR) for mRNA (mRNA) biomarkers or enzyme-linked immunosorbent assay (ELISA) for protein biomarkers.[12,13] Although these methods are the current standards with high specificity and sensitivity, they are disruptive and discontinuous, requiring large amounts of tissue to facilitate experimental sampling and processing to provide temporal information. Alternatively, cell engineering to introduce fluorescent gene reporters allows visualization of marker expression in real-time.[15,16] Such modification, however, suffers from risks of insertional mutagenesis and poor integration efficiency for primary cells, necessitating multiple clonal selections to obtain stable-expressing cell population.[17] Consequently, the process can be labor-intensive and time-consuming. A facile, non-integrative sensor moiety which enables semiquantitative monitoring of tubuloid state in real-time would greatly enhance tubuloid utility in early evaluation of nephrotoxicity in drug development.

Nanoflare (NF), a nanosensor platform based on oligonucleotide-decorated gold nanoparticles (i.e., spherical nucleic acid/SNA), enables intracellular monitoring of mRNA through facile fluorescence observation.[18,19] Besides its use in 2D cell systems, NF technology has been explored to facilitate monitoring in 3D tissue. Recently, we reported the utilization of topically applied NF as early visual indicators of hypertrophic scars and keloids.[20] Nevertheless, NF utility in 3D tissue model is far from being established. Herein, we applied NF to track injury occurring in a kidney tubuloid model, allowing the prediction and assessment of drug nephrotoxicity. As a proof-of-concept, we synthesized NF for mRNA of kidney injury molecule-1 (KIM-1, an established injury marker for proximal tubules[21,22]) to demonstrate the utility of kidney tubuloid system in screening potential nephrotoxicity of anticancer drugs (Figure 1). We initially validated the platform using two drugs with well-known nephrotoxic effects (aristolochic acid (AA) and cisplatin), which we used as positive controls. Thereafter, this platform was utilized to assess semiquantitatively

the nephrotoxicity of 10 anticancer moieties (i.e., nine small molecules and anti-PD-1 checkpoint inhibitor). These drugs included commonly utilized alkylating, antimetabolites, antimicrotubular, and pathway mediator agents. By examining the time-dependent intensity of NF fluorescence, we assessed the severity and the rate by which these drugs induced tubuloid injury, demonstrating the value of the system for identifying human kidney toxicity ex vivo.

We first tested the signal restoration capability of synthesized KIM-1 NF (Cy3-tagged, 550/575 nm) and glyceraldehyde 3-phosphate dehydrogenase (GAPDH) NF (Cy5-tagged, 650/675 nm) in solution. NF fluorescence was measured before and after the addition of equimolar amounts of off-target or complementary target oligonucleotides. As shown in Figure 2a, the fluorescence intensity of both NF solutions increased ~30-fold upon the addition of complementary targets. In comparison, there was only an ~3-fold increase of fluorescence when the off-target oligonucleotides were present. This change could be caused by the charge disruption and partial hybridization to NF by off-target strands. Nonetheless, NF functionality was verified with ~10-fold greater activation from hybridization with the correct target. The storage stability of KIM-1 and GAPDH NFs were also examined by comparing their performance after 1-week storage at 4 °C to that of fresh NFs. As shown in Figure S1, both NFs retained at least 70–80% of original reporting capability. To optimize monitoring performance, freshly prepared NFs were utilized in subsequent studies.

We then studied the applicability of NFs to monitor kidney cells in both 2D and 3D settings. As 2D-seeded proximal tubule cells (PTCs) minimally express KIM-1 mRNA, the specificity of KIM-1 was demonstrated on engineered cell lines or through adenovirus transfection. As shown in Figure 2b, KIM-1 NF fluorescence was observed on LLC-PK1 cells engineered to constitutively express KIM-1 mRNA (KIM-1-PK1), but not in control PK1 cells (PC–PK1). Comparatively, primary human PTCs only exhibited KIM-1 NF fluorescence following infection with adenovirus expressing a KIM-1/enhanced green fluorescence protein (EGFP) construct (Figure 2c). Here, coexpression of KIM-1 NF (Cy3, red) and EGFP (green) in thePTC + Adeno group highlights the KIM-1 NF specificity.

In examining NF performance for 3D kidney tubuloids, we first studied NF distribution in suspended tubuloids having a diameter of ~300–400 μm. The fluorescence signal from GAPDH NF was observed throughout the mature primary tubuloid, with significantly greater intensity than when a scrambled NF (i.e., nontargeted NF) was used (Figure S2). Retention of NF monitoring specificity was corroborated by the coexpression of KIM-1 NF (Cy3, red) and EGFP (green) only on transfected tubuloids (Figure S3). Subsequently, we elevated the KIM-1 expression on primary tubuloids using AA treatment and compared KIM-1 NF expression on these injured tubuloids to those on vehicle-treated tubuloids. As anticipated, strong KIM-1 NF fluorescence was observed in the AA-treated tubuloid (Figure 2d).

Subsequently, NF nanosensors were used to monitor the dynamic changes of cellular KIM-1 mRNA in human kidney tubuloids. To account for heterogeneity in NF uptake between individual tubuloids, we labeled the tubuloids with both KIM-1 Cy3 and GAPDH Cy5 NFs in all subsequent studies. Signal from KIM-1 NF was always normalized against that from

GAPDH NF in performing semiquantitative analysis of tubuloid phenotype (i.e., following injury induction). This normalization was expected to provide more accurate assessment of tubuloid status.[20]

Tubuloids were treated with AA or cisplatin, two well-known nephrotoxic agents as positive controls. The tubuloids were prelabeled with NFs prior to drug treatment and monitored at different time points after treatment for the NF fluorescence signals. As shown in Figure 3a-c, KIM-1 NF fluorescence increased gradually in both AA and cisplatin treated groups. When the AA and cisplatin concentrations were lowered, fluorescent signals from KIM-1 NF were weaker, in accordance with dose-dependency of injury (Figures S4-S6). KIM-1 NF expression in the vehicle-treated group remains comparatively low throughout the 72 h monitoring period (Figure 3a, d). At the end, confocal fluorescence microscopy was performed to examine NF fluorescence distribution in the tubuloid. Thorough cross-sectional NF expression and significant colocalization with nuclear Hoechst33342 staining suggests that NFs are well-internalized, retained, and activated in cells across the tubuloid (Figure 3e). Moreover, confocal microscopy revealed that KIM-1 NF expression in vehicle-treated tubuloids is localized only in the center (red). This slight KIM-1 expression may be primarily attributable to insufficient nutrient exchange in the tubuloid core.

Furthermore, we confirmed the observed KIM-1 NF profiles by evaluating the changes in KIM-1 mRNA expression in the tubuloids post AA or cisplatin-induced injury by qPCR. Overall, 3–6-fold upregulation of cellular KIM-1 mRNA was observed, in a time and dose-dependent fashion. Notably, KIM-1 upregulation occurred sooner for cisplatin treatment (20 and 40 μg/mL), whereas AA treatment (including the 80 μM concentration) resulted in a more gradual upregulation over time (Figure 4a, b). Plotting normalized NF signal to GAPDH signal ratio against its corresponding mRNA expression level, a linear correlation was noted (R^2 = 0.931; Figure 4c). Therefore, KIM-1 NF (with GAPDH NF as normalizing signal) facilitates facile monitoring of KIM-1 mRNA expression, which is upregulated during tubuloid injury. Besides KIM-1 mRNA, we checked another tubular injury biomarker, clusterin (CLU) mRNA. Notwithstanding the slight differences in mRNA fold expressions, CLU upregulation profiles were comparable to those observed for KIM-1 mRNA, further verifying the induced tubuloid injury (Figure S7).

We then examined the potential nephrotoxicity of 10 anticancer chemotherapeutics using the NF-tubuloid platform. Nine small molecule drugs involving several molecular mechanisms (i.e., alkylating, antimetabolites, antimicrotubular, and pathway mediators) were selected and tested for their human kidney tubuloid toxicity alongside the PD-1 checkpoint inhibitor (nivolumab). The complete list of drug name, classification and concentrations tested can be found on Table S1. Anticancer drugs were applied to NF-labeled tubuloids and fluorescence signal expression was monitored as the indicator for injury induction. At each time point, quantified KIM-1 NF signal (Cy3) was normalized to the corresponding GAPDH NF signal (Cy5) and expressed as fold increase over the initial KIM-1 NF/GAPDH NF ratio before any drug treatment. The calculated fold increase was then color coded from blue to red (1–3.5-fold) to prepare the heatmap.

As summarized in the NF fluorescence heatmap in Figure 5a, most drugs exerted significantly less toxicity toward the kidney tubuloids when compared to AA & cisplatin. Observable toxicity (i.e., rate and extent of KIM-1 NF overexpression) was dose-dependent. Moreover, a notable increase of KIM-1 NF signal occurred primarily after 48 h of treatment. To this end, paclitaxel (PTX) was the only exception, with significant KIM-1 NF overexpression induced after 24 h at high dosage (5 μM). 5-Fluorouracil (5-FU) resulted in significant tubuloid injury after 48 h of treatment at 20 μM concentration. In addition, significant KIM-1 NF signal was observed after 72 h at clinically relevant PTX concentrations of 1 and 5 μM. Methotrexate (MTX) also induced noticeable injury after 48 h at 5 and 20 μM concentrations. Of the remaining drugs, cyclophosphamide (CP), pemetrexed (PEM), 5-azacytidine (5-AzaC), nivolumab (Nivo), and imatinib mesylate (IM) induced mild KIM-1 upregulation at 72 h following high dosage treatment (at 1 mM, 50, μM, 20 μM, 2 μM, and 20 μM concentration, respectively). Finally, ifosfamide (IFO) and abemaciclib mesylate (ABM) were the least toxic at the tested concentrations, with negligible impact on KIM-1 tubuloid expression even after 72 h.

To evaluate the accuracy of the generated NF heatmap, we performed qPCR verification on three representative drugs showing severe, mild, and minimal KIM-1 upregulation (PTX, MTX, and ABM at two concentrations each). As shown in Figure 5b-d, NF heatmap (red line) reflects closely the expression profile of tubuloid KIM-1 mRNA (black column) following the drug treatment. Notwithstanding slight deviations, the heatmap values correlate well with mRNA levels from standard qPCR, further demonstrating the accuracy of real-time NF monitoring.

Better tools to predict and assess drug nephrotoxicity using human tissue are critically needed to facilitate drug development and avoid AKI which has high morbidity and mortality and is associated with progression to chronic kidney disease. With steadily increasing development of drugs for multiple human conditions, kidney toxicity assessment remains crucial, and animal models do not always predict adverse effects in humans. Here we have defined a 3D kidney tubuloid monitoring system, consisting of human kidney tubuloids and versatile NF mRNA nanosensors for facile, timely nephrotoxicity assessment. The NF nanosensor enables real-time monitoring of mRNA biomarkers with spatiotemporal information on tubuloid status and functionality (Figure 1), circumventing the delay and challenges associated with major primary cell expansion for large number of cells required in conventional end-point analyses. This approach was first verified using the positive control, tubuloids treated with known nephrotoxicants, cisplatin and AA. The results (3/3.5-fold KIM-1 NF fluorescence) were consistent with the results of qPCR (4.5/5.7-fold KIM-1 mRNA after 72 h at the highest cisplatin & AA concentration, R^2 = 0.931 overall correlation, Figures 3 and 4). It should also be noted that, unlike the conventional qPCR method, which requires pooling of several tubuloids to ensure sufficient mRNA concentration, NF signal profiles individual tubuloids. This allows more accurate identification and consistency of the tubuloid response, while allowing significant resource minimalization.

As an example of the technique's utility, we screened 10 anticancer drugs that are broadly classified based on their mechanism of actions. Alkylating agents (e.g., IFO, CP) and

platinum compounds (e.g., cisplatin) induce DNA damage and cell apoptosis through alkyl group modification[23] and cross-linking.[24] Antimetabolites (e.g., 5-FU) insert false metabolites to interfere with DNA/RNA synthesis and enzymatic activities.[25] Demethylation agents (e.g., 5-AzaC) activate tumor suppressor genes silenced by hypermethylation.[26] Antimicrotubules (e.g., PTX) influence microtubule stability to block cell division.[27] Alternatively, several drugs modulate particular molecular pathways. ABM inhibits cyclin-dependent kinase (CDK)-4/6 to arrest the cell cycle at G1.[28] IM inhibits the aberrant BCR-ABL tyrosine kinase to modulate proliferation and apoptosis.[29] Finally, checkpoint inhibitors (CPIs; e.g., Nivolumab) restore T cells activity against cancer cells presenting blocker ligands.[30]

Considering the distinct therapeutic mechanisms, we chose 1–2 drugs in each class for examination with the NF-tubuloid platform. Our NF heatmap (Figure 5) reveals severe tubuloid injury caused by antimetabolites 5-FU and antimicrotubular PTX, comparable or more than that induced by cisplatin in the clinical concentration range (~4–10 μg/mL). Previous studies have revealed that administration of 5-FU led to severe tubular necrosis, with accompanying intertubular hemorrhage and inflammatory cells infiltration in peritubular spaces.[31] Such injury was attributed to free radicals and cell membrane damage, in addition to DNA/RNA synthesis interference.[32] Similarly, acute PTX nephrotoxicity was previously reported in mice at 0.6 mg/kg dosage, observable at 6 h and increasingly prominent by 24 and 48 h of treatment. Focal necrotic and apoptotic regions were first observed on renal tubules before extending to glomerular atrophy.[33] By comparison, alkylating agents and pathway inhibitors exerted mild toxicity during the three-day monitoring, likely from the accumulated oxidative stresses.[34] By contrast, ABM treatment minimally impacted tubuloid KIM-1 expression, consistent with a previous report in which ABM administration affected tubular secretion and the serum creatinine level, increasing urinary kidney injury markers (KIM-1 and neutrophil gelatinase-associated lipocalin/NGAL).[35]

Consisting of human primarily kidney epithelia, the current system allows monitoring of direct injury, excluding indirect toxicity exerted by drugs (i.e., vascular effects, crystal deposition). Nevertheless, NF-enabled tubuloid injury monitoring is a clinically important approach for facile and timely screening of drug nephrotoxicity. This monitoring platform can predict the risks of severe nephrotoxicity in individuals exposed to therapeutic agents and allows for modification of the environment of the cells such as an increase in uremic solutes or alternation in glucose, lipid or fatty acid environments that will potentially allow for modeling of comorbidities or preexisting kidney conditions, guiding the development of countermeasures to avoid or treat toxicity. Thus, better therapeutic outcomes would be achieved, reducing patient morbidity, healthcare utilization and cost. In the future, this platform can be extended to perform multiplexed monitoring of functional genes, such as dual monitoring of an injury marker with a tubule differentiation marker (to observe dedifferentiation and injury simultaneously), or with a fibrosis marker (to observe acute and chronic nephrotoxicity). Moreover, the facile nature of NF mRNA monitoring warrants adaptation in more complex kidney organoids (presenting other kidney segments) or more broadly in other tissue organoids (e.g., liver and cardiac model) also subjected to prominent drug toxicity.

In summary, we report the facile assessment of drug nephrotoxicity using a clinically applicable NF-tubuloid platform. Development of this platform is inspired by the need for better predictive tools in drug development to assess the likelihood of nephrotoxicity in humans and the potential to personalize therapy by relating genetic makeup to nephrotoxicity susceptibility. Using KIM-1 mRNA as the model nephrotoxicity biomarker, we confirmed the renal toxicity of AA and cisplatin by monitoring the fluorescence signals from KIM-1 NF with GAPDH NF as the internal reference signal. Good linear correlation (R^2 = 0.931) between the NF fluorescence and mRNA expression from qPCR suggests its accuracy. To showcase its eventual adaptation, we then employed the NF-tubuloid platform to study the potential nephrotoxicity of 10 anticancer moieties at varying concentrations. Given its facile labeling and real-time monitoring nature, the system alleviates the problems associated with extrapolation from animal studies or from dedifferentiated 2D human cell models.

Supplementary Material

Refer to Web version on PubMed Central for supplementary material.

ACKNOWLEDGMENTS

C.X. acknowledges the funding support from City University of Hong Kong (#9610472), General Research Fund (GRF) of University Grant Committee of Hong Kong (UGC) Research Grant Council (RGC) (#9042951), and NSFC/RGC Joint Research Scheme (N_CityU118/20). This work was supported by grants to J.V.B. from the US National Institutes of Health/NCATS and NIDDK UH3TR002155, NIDDK 2R01DK072381, and NIDDK R37DK039773. Y.M was supported by Postdoctoral Fellowship from Uehara Memorial Foundation and by Overseas Research Fellowships from Japan Society for the Promotion of Science.

ABBREVIATIONS

5-AzaC	5-azacytidine
5-FU	5-fluorouracil
AA	aristolochic acid
ABM	abemaciclib mesylate
AKI	acute kidney injury
Cisp	cisplatin
CLU	clusterin
CP	cyclophosphamide
EGFP	enhanced green fluorescence protein
ELISA	enzyme-linked immunosorbent assay
GAPDH	glyceraldehyde 3-phosphate dehydrogenase
IFO	ifosfamide

IM	imatinib mesylate
KIM-1	kidney injury molecule 1
MTX	methotrexate
NF	nanoflare
NGAL	neutrophil gelatinase-associated lipocalin
Nivo	nivolumab
PEM	pemetrexed
PTC	proximal tubule cell
PTX	paclitaxel
RT-qPCR	real-time quantitative polymerase chain reaction
SNA	spherical nucleic acid

REFERENCES

(1). O'Neal JB; Shaw AD; Billings FT Acute kidney injury following cardiac surgery: current understanding and future directions. Crit. Care 2016, 20 (1), 1–9. [PubMed: 26728475]

(2). Faria J; Ahmed S; Gerritsen KG; Mihaila SM; Masereeuw R Kidney-based in vitro models for drug-induced toxicity testing. Arch. Toxicol 2019, 93, 3397–3418. [PubMed: 31664498]

(3). Perazella MA; Moeckel GW In Nephrotoxicity from chemotherapeutic agents: clinical manifestations, pathobiology, and prevention/therapy. Semin. Nephrol 2010, 30, 570–581. [PubMed: 21146122]

(4). Horie S; Oya M; Nangaku M; Yasuda Y; Komatsu Y; Yanagita M; Kitagawa Y; Kuwano H; Nishiyama H; Ishioka C; et al. Guidelines for treatment of renal injury during cancer chemotherapy 2016. Clin. Exp. Nephrol 2018, 22 (1), 210–244. [PubMed: 28856465]

(5). Ferenbach DA; Bonventre JV Mechanisms of maladaptive repair after AKI leading to accelerated kidney ageing and CKD. Nat. Rev. Nephrol 2015, 11 (5), 264–276. [PubMed: 25643664]

(6). Yu S M-W; Bonventre JV Acute Kidney Injury and Maladaptive Tubular Repair Leading to Renal Fibrosis. Curr. Opin. Nephrol. Hypertens 2020, 29 (3), 310–318. [PubMed: 32205583]

(7). Cosmai L; Porta C; Foramitti M; Perrone V; Mollica L; Gallieni M; Capasso G Preventive strategies for acute kidney injury in cancer patients. Clin. Kidney J 2021, 14 (1), 70–83. [PubMed: 33564407]

(8). Bonventre JV Kidney organoids-a new tool for kidney therapeutic development. Kidney Int. 2018, 94, 1040–1042. [PubMed: 30466559]

(9). Yousef Yengej FA; Jansen J; Rookmaaker MB; Verhaar MC; Clevers H Kidney Organoids and Tubuloids. Cells 2020, 9, 1326. [PubMed: 32466429]

(10). Morizane R; Lam AQ; Freedman BS; Kishi S; Valerius MT; Bonventre JV Nephron organoids derived from human pluripotent stem cells model kidney development and injury. Nat. Biotechnol 2015, 33 (11), 1193–1200. [PubMed: 26458176]

(11). Schutgens F; Rookmaaker MB; Margaritis T; Rios A; Ammerlaan C; Jansen J; Gijzen L; Vormann M; Vonk A; Viveen M; Yengej FY; Derakhshan S; de Winter-de Groot KM; Artegiani B; van Boxtel R; Cuppen E; Hendrickx APA; van den Heuvel-Eibrink MM; Heitzer E; Lanz H; Beekman J; Murk JL; Masereeuw R; Holstege F; Drost J; Verhaar MC; Clevers H Tubuloids derived from human adult kidney and urine for personalized disease modeling. Nat. Biotechnol 2019, 37, 303–313. [PubMed: 30833775]

(12). Mori Y; Ajay AK; Chang J-H; Mou S; Zhao H; Kishi S; Li J; Brooks CR; Xiao S; Woo H-M; et al. KIM-1 mediated tubular fatty acid uptake leads to progressive diabetic kidney disease. Cell Metab. 2021, 33 (5), 1042–1061.e7. [PubMed: 33951465]

(13). Jamalpoor A; van Gelder CA; Yengej FAY; Zaal EA; Berlingerio SP; Veys KR; Casellas CP; Voskuil K; Essa K; Ammerlaan CM; Rega LR; van der Welle R; Lilien MR; Rookmaaker MB; Clevers H; Klumperman J; Levtchenko E; Berkers CR; Verhaar MC; Altelaar M; Masereeuw R; Janssen MJ Cysteamine-bicalutamide combination treatment restores alpha-ketoglutarate and corrects proximal tubule phenotype in cystinosis. bioRxiv 2020, 941799. https://www.biorxiv.org/content/10.1101/2020.02.10.941799v1 (accessed 2021-06-09).

(14). Zink D; Chuah JKC; Ying JY Assessing toxicity with human cell-based in vitro methods. Trends Mol. Med 2020, 26 (6), 570–582. [PubMed: 32470384]

(15). Howden SE; Vanslambrouck JM; Wilson SB; Tan KS; Little MH Reporter-based fate mapping in human kidney organoids confirms nephron lineage relationships and reveals synchronous nephron formation. EMBO Rep. 2019, 20, No. e47483. [PubMed: 30858339]

(16). Jung KB; Lee H; Son YS; Lee JH; Cho H-S; Lee MO; Oh J-H; Lee J; Kim S; Jung CR; Kim J; Son M-Y In vitro and in vivo imaging and tracking of intestinal organoids from human induced pluripotent stem cells. FASEB J. 2018, 32, 111–122. [PubMed: 28855280]

(17). Nienhuis AW; Dunbar CE; Sorrentino BP Genotoxicity of retroviral integration in hematopoietic cells. Mol. Ther 2006, 13 (6), 1031–1049. [PubMed: 16624621]

(18). Randeria PS; Briley WE; Chinen AB; Guan CM; Petrosko SH; Mirkin CA, Nanoflares as probes for cancer diagnostics. In Nanotechnology-Based Precision Tools for the Detection and Treatment of Cancer; Springer: New York City, 2015; pp 1–22.

(19). Li J; Wang J; Liu S; Xie N; Quan K; Yang Y; Yang X; Huang J; Wang K Amplified FRET Nanoflares: An Endogenous mRNA-Powered Nanomachine for Intracellular MicroRNA Imaging. Angew. Chem 2020, 132 (45), 20279–20286.

(20). Yeo DC; Wiraja C; Paller AS; Mirkin CA; Xu C Abnormal scar identification with spherical-nucleic-acid technology. Nat. Biomed. Eng 2018, 2 (4), 227–238. [PubMed: 30936446]

(21). Han WK; Bailly V; Abichandani R; Thadhani R; Bonventre JV Kidney Injury Molecule-1 (KIM-1): a novel biomarker for human renal proximal tubule injury. Kidney Int. 2002, 62 (1), 237–244. [PubMed: 12081583]

(22). Ichimura T; Asseldonk EJ; Humphreys BD; Gunaratnam L; Duffield JS; Bonventre JV Kidney injury molecule-1 is a phosphatidylserine receptor that confers a phagocytic phenotype on epithelial cells. J. Clin. Invest 2008, 118 (5), 1657–1668. [PubMed: 18414680]

(23). Lajous H; Lelièvre B; Vauléon E; Lecomte P; Garcion E Rethinking alkylating (-like) agents for solid tumor management. Trends Pharmacol. Sci 2019, 40 (5), 342–357. [PubMed: 30979523]

(24). Hato SV; Khong A; de Vries IJM; Lesterhuis WJ Molecular pathways: the immunogenic effects of platinum-based chemotherapeutics. Clin. Cancer Res 2014, 20 (11), 2831–2837. [PubMed: 24879823]

(25). Valenzuela MMA; Neidigh JW; Wall NR Antimetabolite treatment for pancreatic cancer. Chemotherapy 2014, 3 (3), 137. [PubMed: 26161298]

(26). Müller A; Florek M, 5-Azacytidine/Azacitidine. In Small Molecules in Oncology; Martens U, Ed.; Recent Results in Cancer Research; Springer: Berlin, 2010; Vol. 184, pp 159–170.

(27). Garbe C Antimicrotubule Agents. In Dermatologic Principles and Practice in Oncology; Lacouture ME, Ed.; John Wiley & Sons: Hoboken, NJ, 2013; pp 208–214.

(28). Corona SP; Generali D Abemaciclib: a CDK4/6 inhibitor for the treatment of HR+/HER2− advanced breast cancer. Drug Des., Dev. Ther 2018, 12, 321–330.

(29). Marcucci G; Perrotti D; Caligiuri MA Understanding the Molecular Basis of Imatinib Mesylate Therapy in Chronic Myelogenous Leukemia and the Related Mechanisms of Resistance. Clin. Cancer Res 2003, 9 (4), 1248–1252. [PubMed: 12684391]

(30). Alsaab HO; Sau S; Alzhrani R; Tatiparti K; Bhise K; Kashaw SK; Iyer AK PD-1 and PD-L1 Checkpoint Signaling Inhibition for Cancer Immunotherapy: Mechanism, Combinations, and Clinical Outcome. Front. Pharmacol 2017, 8, 561. [PubMed: 28878676]

(31). Rashid S; Ali N; Nafees S; Hasan SK; Sultana S Mitigation of 5-Fluorouracil induced renal toxicity by chrysin via targeting oxidative stress and apoptosis in wistar rats. Food Chem. Toxicol 2014, 66, 185–193. [PubMed: 24486618]

(32). Yousef HN; Aboelwafa HR The potential protective role of taurine against 5-fluorouracil-induced nephrotoxicity in adult male rats. Exp. Toxicol. Pathol 2017, 69 (5), 265–274. [PubMed: 28189472]

(33). Rabah SO Acute Taxol nephrotoxicity: Histological and ultrastructural studies of mice kidney parenchyma. Saudi J. Biol. Sci 2010, 17 (2), 105–114. [PubMed: 23961065]

(34). Ensergueix G; Pallet N; Joly D; Levi C; Chauvet S; Trivin C; Augusto J-F; Boudet R; Aboudagga H; Touchard G; Nochy D; Essig M; Thervet E; Lazareth H; Karras A Ifosfamide nephrotoxicity in adult patients. Clin. Kidney J 2020, 13 (4), 660–665. [PubMed: 32897279]

(35). Chappell JC; Turner PK; Pak YA; Bacon J; Chiang AY; Royalty J; Hall SD; Kulanthaivel P; Bonventre JV Abemaciclib Inhibits Renal Tubular Secretion Without Changing Glomerular Filtration Rate. Clin. Pharmacol. Ther 2019, 105 (5), 1187–1195 [PubMed: 30449032]

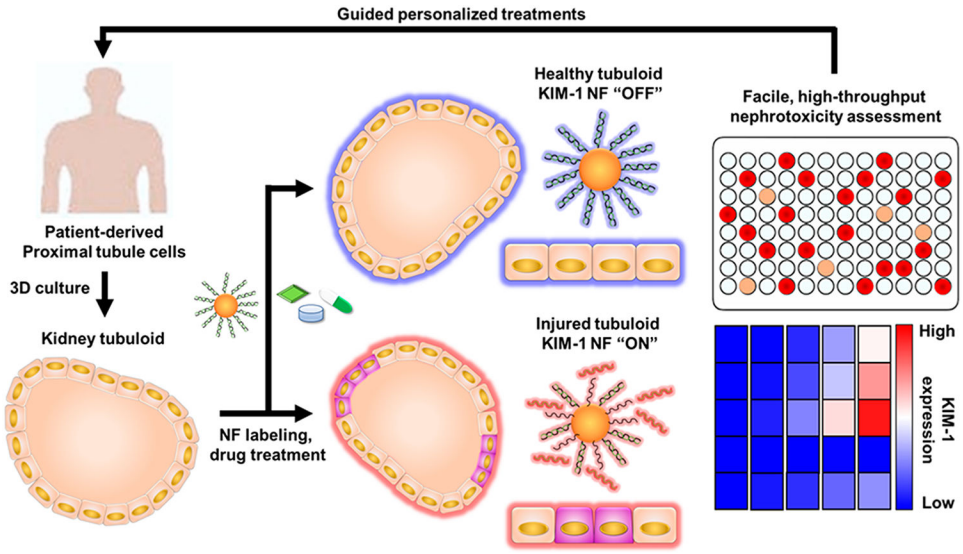

Figure 1.

Schematic illustration showing KIM-1 NF-assisted nephrotoxicity assessment using patient-derived kidney tubuloids. Kidney tubuloids phenocopy physiological proximal tubule functions as an alternative to 2D cultured cells or complex kidney organoids. Facile, real-time monitoring of tubuloid injury through KIM-1 NF expression translates to resource minimization, alleviating the problem of limited patient-derived cell numbers and challenging cell expansion. This personalized nephrotoxicity assessment platform can assist the development and utilization of kidney-safe therapeutics.

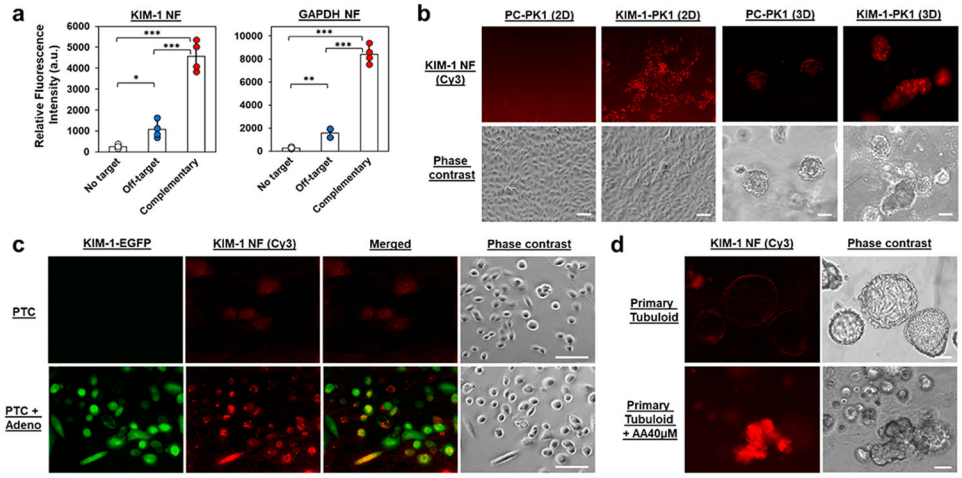

Figure 2.

Examination of the specificity and cellular uptake of NF nanosensors. (a) Hybridization assay of KIM-1 and GAPDH NFs with complementary target and off-target oligonucleotides. (b) KIM-1 NFs detected KIM-1 expression in KIM-1-PK1 cells (constitutive expression of KIM-1 mRNA) but not in the control PC–PK1 cells. (c) Detection of KIM-1 mRNA in primary PTCs following adenoviral infection of KIM-1/EGFP plasmid construct using KIM-1 NFs. EGFP and KIM-1 NF signals were compared in non-infected and adenoviral infected cells. (d) Examination of primary tubuloids following injury after 72 h AA treatment (40 μM) using KIM-1 NFs. Scale bar: 100 μm. *, $p < 0.05$; **, $p < 0.01$; ***, $p < 0.001$. $N = 4$.

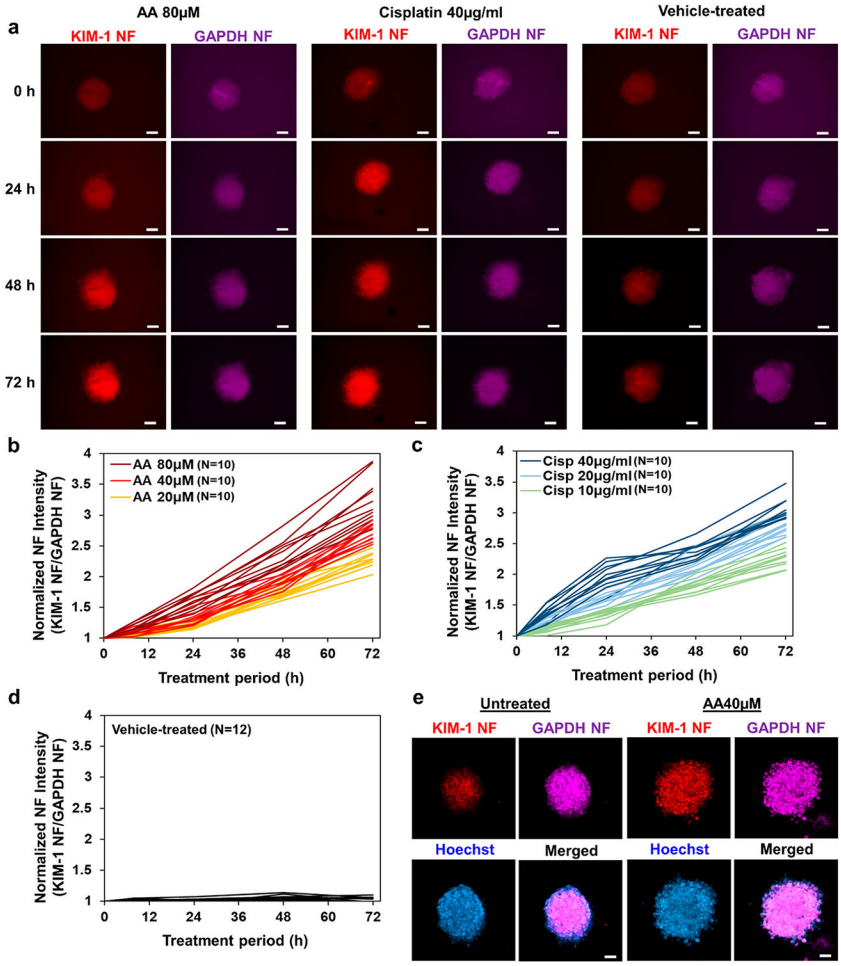

Figure 3.

Real-time assessment of AA/cisplatin induced injury in primary kidney epithelial cell tubuloids. (a) Representative images showing AA-treated, cisplatin-treated, and vehicle-treated tubuloids that were prelabeled with KIM-1 Cy3 NF (red) and GAPDH Cy5 NF (purple). NF signal profiles of (b) AA-treated tubuloids (20, 40, 80 μM concentrations, $N = 10$ each), (c) cisplatin-treated tubuloids (10, 20, 40 μg/mL concentration, $N = 10$ each), and (d) vehicle-treated tubuloids ($N = 12$). (e) Representative confocal images showing NF fluorescence of vehicle-treated tubuloid (left) and 72 h AA-treated tubuloid (right) prelabeled with KIM-1 Cy3 NF (red), GAPDH Cy5 NF (purple), and stained with Hoechst33342 (blue). Scale bar: 100 μm.

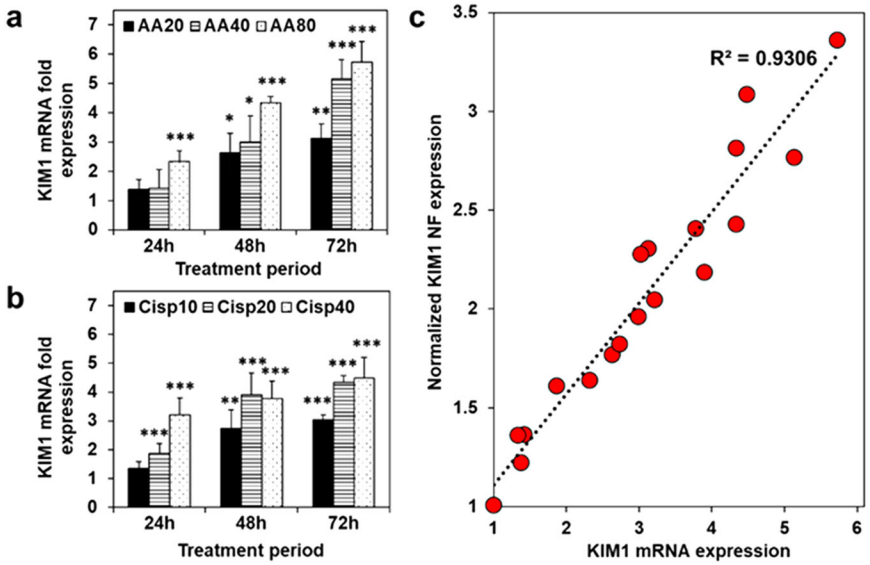

Figure 4.

qPCR quantification of cellular KIM-1 mRNA in the tubuloids treated with (a) aristolochic acid (AA) and (b) cisplatin (Cisp) for 24, 48, or 72 h at three designated concentrations. (c) Normalized NF expression (KIM-1 NF signal normalized by GAPDH NF) plotted against corresponding KIM-1 mRNA expression in a and b shows linear correlation. *, $p < 0.05$; **, $p < 0.01$; ***, $p < 0.001$ to vehicle-treated tubuloids. $N = 6$.

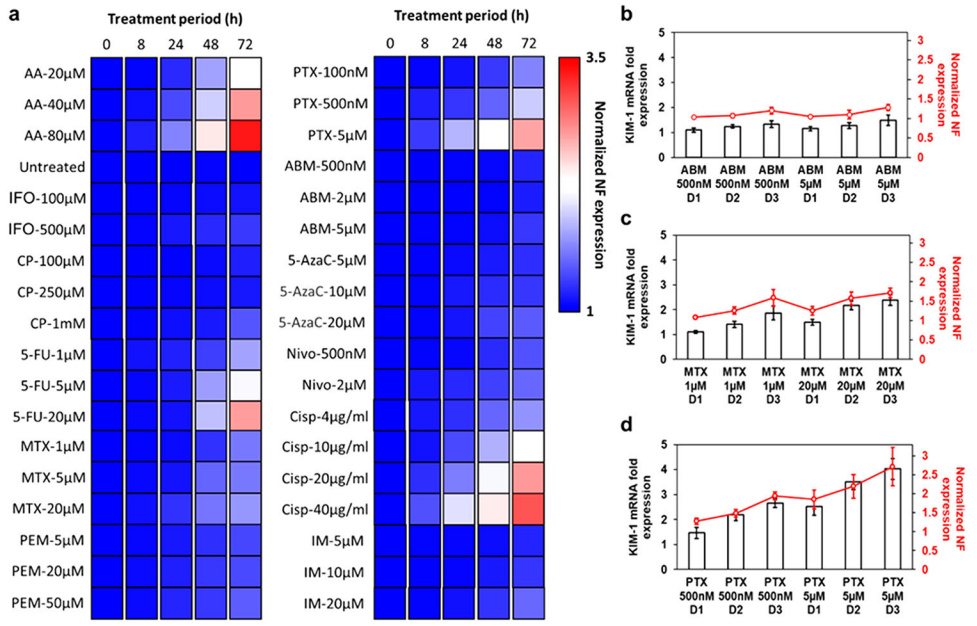

Figure 5.

KIM-1 NF signal profile on primary kidney epithelial tubuloids following treatment with 10 anticancer drugs. (a) Heatmap showing normalized KIM-1 NF expression after 8, 24, 48, or 72 h of drug treatments ($N = 6$). Column-line plot showing correlation between KIM-1 NF expression (red line) and KIM-1 mRNA fold expression (black bars) after the treatment with (b) ABM (500 nM and 5 μM), (c) MTX (1 and 20 μM), or (d) PTX (500 nM and 5 μM). $N = 6$.